Cognitive Neuropsychology

ISSN: 0264-3294 (Print) 1464-0627 (Online) Journal homepage: https://www.tandfonline.com/loi/pcgn20

Separating neural correlates of allocentric and egocentric neglect: Distinct cortical sites and common white matter disconnections

Magdalena Chechlacz , Pia Rotshtein , Wai-Ling Bickerton , Peter C. Hansen , Shoumitro Deb & Glyn W. Humphreys

To cite this article: Magdalena Chechlacz , Pia Rotshtein , Wai-Ling Bickerton , Peter C. Hansen , Shoumitro Deb & Glyn W. Humphreys (2010) Separating neural correlates of allocentric and egocentric neglect: Distinct cortical sites and common white matter disconnections, Cognitive Neuropsychology, 27:3, 277-303, DOI: 10.1080/02643294.2010.519699

To link to this article: https://doi.org/10.1080/02643294.2010.519699

COGNITIVE NEUROPSYCHOLOGY, 2010, 27 (3), 277–303

Psychology Press
Taylor & Francis Group

Separating neural correlates of allocentric and egocentric neglect: Distinct cortical sites and common white matter disconnections

Magdalena Chechlacz, Pia Rotshtein, Wai-Ling Bickerton, Peter C. Hansen, Shoumitro Deb, and Glyn W. Humphreys

Behavioural Brain Sciences Centre, School of Psychology, University of Birmingham, Birmingham, UK

Insights into the functional nature and neuroanatomy of spatial attention have come from research in neglect patients but to date many conflicting results have been reported. The novelty of the current study is that we used voxel-wise analyses based on information from segmented grey and white matter tissue combined with diffusion tensor imaging to decompose neural substrates of different neglect symptoms. Allocentric neglect was associated with damage to posterior cortical regions (posterior superior temporal sulcus, angular, middle temporal and middle occipital gyri). In contrast, egocentric neglect was associated with more anterior cortical damage (middle frontal, postcentral, supramarginal, and superior temporal gyri) and damage within subcortical structures. Damage to intraparietal sulcus (IPS) and the temporo-parietal junction (TPJ) was associated with both forms of neglect. Importantly, we showed that both disorders were associated with white matter lesions suggesting damage within long association and projection pathways such as the superior longitudinal, superior fronto-occipital, inferior longitudinal, and inferior fronto-occipital fascicule, thalamic radiation, and corona radiata. We conclude that distinct cortical regions control attention (a) across space (using an egocentric frame of reference) and (b) within objects (using an allocentric frame of reference), while common cortical regions (TPJ, IPS) and common white matter pathways support interactions across the different cortical regions.

Keywords: Visual neglect; Spatial attention; Allocentric; Egocentric; Diffusion tensor imaging; Voxel-based morphometry.

Patients with unilateral visual neglect fail to attend to stimuli presented on the side of space contralateral to their lesion (Heilman & Valenstein, 1979). These patients provide an important source of evidence about the brain regions necessary to the allocation of attention to space. The nature of the "space" that is neglected may vary across patients. For example, some patients demonstrate neglect based on where stimuli fall in relation to their body (egocentric neglect; Doricchi & Galati,

Correspondence should be addressed to Magdalena Chechlacz, Behavioural Brain Sciences Centre, School of Psychology, University of Birmingham, Edgbaston, Birmingham B15 2TT, UK (Email: mxc673@bham.ac.uk).

This work was supported by grants from the Medical Research Council, the Leverhulme Trust (to P.R.), and the Stroke Association (UK).

http://www.psypress.com/cogneuropsychology DOI:10.1080/02643294.2010.519699

2000; Riddoch & Humphreys, 1983), while others neglect parts that fall on the contralesional side of objects irrespective of the positions of the objects relative to the patient (allocentric neglect; Doricchi & Galati, 2000; Kleinman et al., 2007; Olson, 2003; Walker, Findlay, Young, & Lincoln, 1996; Walker & Young, 1996). Egocentric and allocentric neglect can dissociate across patients (Marsh & Hillis, 2008) and can even occur on opposite sides of space within single patients with bilateral brain lesions (Humphreys & Riddoch, 1994, 1995). Understanding the neural regions that control spatial attention may depend on separating the circuits supporting the attention (a) across space in relation to the body and (b) across parts within objects.

There have been several prior attempts to use data from neglect patients to make inferences about the neural substrates of spatial attention, and the results have proved controversial. Some findings suggest that damage to the temporo-parietal junction (TPJ) is critical in developing neglect syndrome (Leibovitch et al., 1998; Vallar, 2001; Vallar, Bottini, & Paulesu, 2003). A second line of studies report that lesions to the superior temporal gyrus (STG) insula, pulvinar, and basal ganglia are crucial (Karnath, 2001; Karnath, Ferber, & Himmelbach, 2001; Karnath, Fruhmann Berger, Kuker, & Rorden, 2004a; Karnath, Himmelbach, & Rorden, 2002; Karnath et al., 2005). A third set of findings highlights damage to angular gyrus and the medial temporal lobe (parahippocampus; Mort et al., 2003). Finally, some researchers have tried to resolve the controversies on critical cortical regions associated with neglect by suggesting that neglect is a disconnection syndrome (Bartolomeo, Thiebaut de Schotten, & Doricchi, 2007; Doricchi & Tomaiuolo, 2003). This hypothesis is supported by findings from single case studies (Thiebaut de Schotten et al., 2005; Urbanski et al., 2008) and pathway-of-interest analyses (Bird et al., 2006; He et al., 2007; Thiebaut de Schotten et al., 2008; Thiebaut de Schotten et al., 2005; Urbanski et al., 2008) showing that neglect is associated with damage to the superior longitudinal fasciculus (SLF; He et al., 2007; Thiebaut de Schotten et al., 2008), the inferior longitudinal fasciculus (ILF; Bird et al., 2006), and the inferior fronto-occipital fasciculus (IFOF; Urbanski et al., 2008). Thus, taken together, prior neuroanatomical analyses are unclear about the neural substrates of neglect and, consequently, about the neural areas necessary to the control of spatial attention. Previous studies have also not provided comprehensive information about the extent of grey versus white matter contributions to the functional deficits apparent in neglect patients.

One potential explanation for inconsistencies in the literature is that most studies have ignored the heterogeneous nature of the deficit whilst using different behavioural measures to define neglect. For example, in some studies neglect has been defined largely in terms of either performance on line bisection tasks or deficits pooled across line bisection and cancellation (Bird et al., 2006; Mannan et al., 2005; Mort et al., 2003), while in others neglect has been defined using a battery of tasks but all including some degree of spatial exploration (Karnath et al., 2004a; Karnath et al., 2002). While exploration tasks such as line cancellation require that multiple stimuli are coded in relation to the patient (e.g., using an egocentric reference frame), tasks such as line bisection could reflect either separate coding of the perceived ends of the lines in relation to the patient (i.e., egocentric spatial coding) or perception of the line as a single object (i.e., allocentric spatial coding), which make it less clear how a deficit may arise in a given patient (Humphreys & Riddoch, 1994, 1995).

Vallar and colleagues (Vallar et al., 2003) propose that spatial coding within an allocentric frame of reference depends on processing in the ventral visual stream while egocentric spatial coding operates within the dorsal visual stream. Data from single case studies, however, suggest that allocentric neglect may link to damage in both dorsal (occipital-parietal) and ventral (occipital-temporal) areas (Doricchi & Galati, 2000; Walker et al., 1996; Walker & Young, 1996). There have been previous attempts to distinguish the neuroanatomical basis of these putative forms of neglect using groups of patients. Following

Binder, Marshall, Lazar, Benjamin, and Mohr's (1992) suggestion that different neglect symptoms may be associated with damage to discrete brain areas, Rorden, Fruhmann Berger, and Karnath (2006) compared neglect patients diagnosed from cancellation tests with and without additional line bisection deficits and found that additional poor performance on line bisection was associated with relatively more posterior brain lesions (Binder et al., 1992; Rorden et al., 2006). These two prior studies hypothesized that performance on line bisection and cancellation tasks represent two types of neglect. As we have noted, it is not clear that this is necessarily the case. Moreover, the contrast involved comparing patients with problems on bisection plus cancellation relative to those with problems on cancellation alone. This leaves open the possibility that any contrast reflects the magnitude of the problem, not a difference between different types of neglect. Therefore, this fails to establish whether there are distinct patient groups or whether patients with additional deficits have larger lesions. In addition to this, Rorden et al. (2006) used data derived from a preselected group of 22 patients with left spatial neglect following right brain lesions; it is not clear from this whether the lesions separate these patients from "control" patients, who might have similar lesions but do not present with neglect.

Hillis et al. (2005) reported that abnormalities in the right superior temporal gyrus (STG) were associated with allocentric neglect while damage to the right angular gyrus was linked to egocentric neglect. Medina et al. (2009) argued that egocentric neglect is associated with abnormal function within the supramarginal and superior temporal gyri, while allocentric neglect is associated with dysfunction of middle-superior occipital regions and posterior temporal cortices. Unfortunately the functional contribution of the STG is inconsistent across these studies reported by the same research group, while the contribution of the angular and supramarginal gyri to egocentric neglect did not replicate. One advantage of these two reports lies in their use of different imaging modalities, including perfusion and diffusion imaging, the application of a comprehensive battery of neglect tests suitable for contrasting different neglect symptoms, and inclusion of a large number of patients (50 and 171, respectively)—though the studies were limited to patients with ischemic infarct within the right hemisphere. Both studies relied largely on manual delineation of the abnormal tissue, and demarcation of a lesion was done on a different brain template without applying any formal registration procedure. Such protocols are not only labour intensive but also susceptible to individual biases and uncertainties in mapping as it is not always clear where a lesion starts and ends and how to map the lesion location onto the template. A further limitation of using manual lesion delineation is that it does not capture changes in brain tissue due to atrophy, which may be important given that age influences the severity of neglect following stroke (Gottesman et al., 2008). In addition, the spatial resolution of the main analyses was defined categorically by different Brodmann areas, masking potential functional dissociations within a single area and by including only patients with ischemic infarct confined to right hemisphere. One further point is that there were no formal statistical comparisons between the two types of neglect, and the analysis was restricted to abnormalities of the grey matter. Thus information about the contribution of damage in white matter to the different neglect symptoms is still unclear.[1]

[1] Other potential limitations of previous studies are (a) biased patient selection (based on behaviour or lesion location) and (b) the analyses that were conducted on the neuroimaging data. In particular, earlier studies have used categorical distinctions between patients with and without neglect and thus fail to reflect the severity of the problems in different patients. Furthermore, lesion demarcations have been performed manually in an observer-dependent manner using different template images and different registration and normalization protocols (Karnath, Fruhmann Berger, Zopf, & Kuker, 2004b; Mort et al., 2004; Mort et al., 2003). This introduces a researcher confound in registration and normalization. Manual delineations also typically do not include tissue atrophy and other age-related changes along with the lesion, making the analyses insensitive to the contribution of such structural changes to the functional deficit in patients (Gottesman et al., 2008).

In one other study distinguishing between different neglect symptoms, Verdon, Schwartz, Lovblad, Hauert, and Vuilleumier (2010) argued for three components within the syndrome: (a) a perceptual deficit (assessed through tasks such as text reading and line bisection), (b) a component reflecting attention within an allocentric reference frame (missing the contralesional side of words, missing a contralesional gap in circles), and (c) a component reflecting exploration in egocentric space (missing complete targets on the contralesional side of a page). In contrast to studies relying solely on reduction approaches to behavioural data (i.e., categorically dividing patients to those with neglect and those without neglect), these authors employed observer-dependent lesion demarcations but used voxel-based lesion–symptom mapping based on continuous behavioural scores alongside traditional statistical comparison between lesions in different categorically defined groups. Subsequently they linked the different neglect deficits to (a) the right inferior parietal lobe, (b) lesions to inferior temporal regions, and (c) the right dorsolateral prefrontal cortex. The site linked to allocentric lesions was difficult to establish, however, with the main peak occurring in white matter. Moreover these authors did not directly examine white matter versus grey matter contributions to different components of the neglect syndrome, nor did they use targeted diffusion tensor imaging (DTI) analyses to assess the integrity of specific white matter tracts (though they noted that damage to white matter tracts was likely to be associated with severe neglect).

In the current study we attempted to go beyond these previous lesion–symptom analyses in several ways, but most notably by combining voxel-based analyses with DTI imaging of white matter tracts, along with using behavioural measures from a single task sensitive to both egocentric and allocentric neglect symptoms. Using these combined procedures, we aimed to delineate common and dissociable brain structures involved in allocentric and egocentric neglect, dissociating the contribution of white as well as grey matter changes. Importantly, we used observer-independent voxel-based analysis combined with robust statistical methods to assess the association between the behavioural deficits and the underpinning grey and white matter lesions. We also used both parametric and non-parametric approaches, enabling a comparison to be made between these methods. In addition, we tested allocentric and egocentric neglect in patients with chronic deficits, when patterns of impairment are stabilized after any secondary damage and reorganization of neuronal networks. Our study contrasts with previous reports not only in terms of our image analysis methods but also in employing an unbiased sample (patients were not preselected based on clinical, anatomical, and neuropsychological criteria), and we looked for common structure–function relationships across the whole brain, irrespective of aetiology (stroke, degenerative changes). The whole-brain methods give us an opportunity to incorporate age-related changes such as atrophy into the analysis of the syndrome. The overall approach enables us to ask a question different to that posed hitherto, about what neuronal substrates are necessary to the allocation of attention to allocentric and egocentric space rather than confining our question to the neuropathology of neglect following stroke.

The severity of neglect symptoms here was assessed using a theoretically motivated behavioural test similar to that used by Ota, Fujii, Suzuki, Fukatsu, and Yamadori (2001) in order to simultaneously distinguish allocentric and egocentric neglect. This allowed us to control for variability in patients' behaviour due to differential task demands, test conditions, and stimuli that could potentially arise when using measures of the two types of neglect in different tasks. In addition, the analysis treated the behavioural measurements as continuous variables rather than as categorical scores, which increased both the ability to tease apart the two different types of neglect and the sensitivity for detecting brain–behaviour associations.

Finally, white matter deficits have only been analysed previously using small groups of individuals, pathway of interest analysis, and/or having been looked at separately from grey matter

lesions. We present the first group-level analysis of white matter changes, and, by characterizing both white and grey matter damage, we are able to review the relations between each type of change and how any lesions may link to contrasting forms of neglect. We highlight both common and distinct areas of cortical and subcortical lesions associated with allocentric and egocentric neglect, along with common white matter damage across all neglect patients. The relations between these deficits and multicomponent accounts of visual neglect are discussed in relation to an overall computational framework for understanding spatial selection and neglect.

Method

Participants

A total of 41 patients were recruited for this study (30 males and 11 females), with ages ranging from 32 to 85 years (mean age 63 years). All patients had acquired brain lesions (stroke, carbon monoxide poisoning, degenerative changes), were at a chronic stage (>9 months post injury), and had no contraindications to magnetic resonance imaging (MRI) scanning. No other exclusion criteria were used. All patients participating in this study were recruited from the panel of neuropsychological volunteers established in the Behavioural Brain Sciences Centre at the School of Psychology, University of Birmingham, and all patients had been subject to the Birmingham University Cognitive Screen (BUCS). All patients but 4 had normal or corrected-to-normal vision. Clinical and demographic data for all the patients are shown in Appendix A. These data include analyses demonstrating the test/retest reliability of the measures of neglect, along with the common pattern of deficits found when converging measures of allocentric and egocentric neglect were taken. Two patients had left visual field deficits, and 2 had right visual field deficits. However, as eye and head movements were not restricted in the behavioural task, we included the data from these patients. As listed in Appendix A 3 patients had lesions caused by carbon monoxide poisoning, and 5 patients had chronic degenerative changes. For the purpose of neuroimaging analyses, we excluded the 3 patients with carbon monoxide poisoning.[2]

In addition, for the lesion reconstruction protocol (see below) we acquired T1 weighted images from 73 healthy controls (40 males and 33 females, mean age 61 years, range 30–87) who had no history of stroke, brain damage, or neurological disorders. All participants provided written informed consent in agreement with ethics protocols at the School of Psychology and Birmingham University Imaging Centre (BUIC).

Cognitive assessment

The neglect assessment was based on Apple Cancellation Task developed as a part of Birmingham University Cognitive Screen (BUCS; retrieved August 1, 2010, from http://www.bucs.bham.ac.uk). The Apple Cancellation Task (Figure 1A) is similar to the gap detection task of Ota et al. (2001) and is designed to simultaneously measure egocentric and allocentric neglect. Participants are presented with a page (A4) with 50 apples divided into 5 invisible columns, one middle, one near left, one far left, one near right and one far right. Each column contains 10 complete apples (targets) along with distractors, which are apples with either a left or

[2] One potential weakness with the present approach is that the analysis of the grey matter was based on T1 weighted images. This may underestimate the extent of brain changes (e.g., in acute cases or in patients with carbon monoxide poisoning or degenerative changes). However, all patients included in this study were chronic, and, out of 41 patients, only 3 suffered from carbon monoxide poisoning and 5 from degenerative changes (3 of these patients also suffered from different forms of unspecified vascular disease causing additional acquired brain lesions). Three patients with carbon monoxide poisoning were excluded from neuroimaging analyses. All 5 chronic patients with degenerative changes had defined lesions visible on T1 scan. Furthermore, for most of these patients we have available FLAIR (fluid-attenuated inversion recovery) or T2 contrast images, and the lesion segmentations and reconstructions based on T1 images have been successfully verified based on FLAIR/T2 contrast (see example in Appendix B, Figure B1, B and C). Importantly, note that for the white matter we presented voxel-based morphometry (VBM)-style analyses from DTI images (using T2-based contrast images) that confirm the T1 findings.

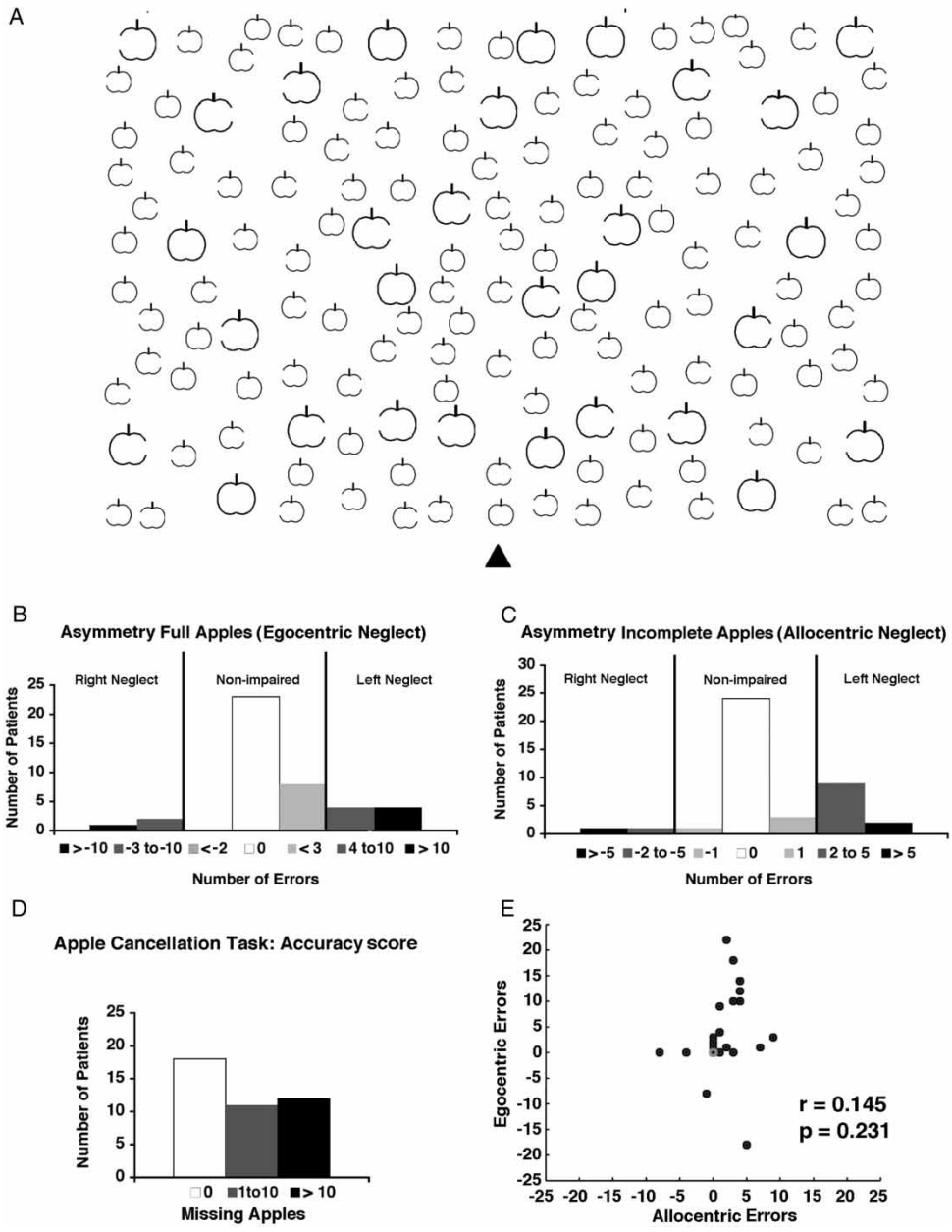

Figure 1. *The Apple Cancellation Task and behavioural results. (A) Copy of the page with apples used in the Apple Cancellation Task. In this test patients are asked to cross all full apples. Egocentric neglect is then measured by whether patients miss targets (full apples) predominantly on one side of the page, and allocentric neglect is measured by whether patients make false-positive responses by cancelling predominantly left or right distractors (i.e., incomplete apples; for full details and scoring see Method section). Patients' performance on the Apple Cancellations Task: (B) asymmetry score for full apples used as criterion of egocentric neglect; (C) asymmetry score for incomplete apples used as criterion of allocentric neglect; and (D) accuracy score. (E) Scatterplot of patients' egocentric neglect errors against patients' allocentric neglect errors on the Apple Cancellation Task. There was no significant correlation between allocentric and egocentric neglect scores. Please note that the middle grey dot corresponds to results for nonimpaired patients.*

a right part missing (incomplete apples). Each column is further subdivided into 2 rows (upper and lower parts), and similar numbers of the three types of items (targets and two types of distractors) are present in the upper and lower sections of each column. A page is placed in landscape orientation in the participant's midline. Participants are given 5 minutes and are instructed to cross out full apples only. Two practice trials are given before testing.

The maximum achievable score in the Apple Cancellation Task is 50. Egocentric neglect is determined by whether patients miss targets (complete apples) on the left or right side of the page. Allocentric neglect is determined by whether patients make false-positive responses by cancelling incomplete apples (distractors) where the gap is on either the right or left side of each apple, irrespective of the position of the (incomplete) apple on the page. Cut-offs to classify patients as having egocentric or allocentric neglect were calculated on the basis of asymmetry scores (left- vs. right-side egocentric or allocentric errors), using scores from 86 elderly control participants with no history of neurological diseases (35 males and 51 females, mean age 67 years, range 47–88), and were as follows: egocentric asymmetry for full apples (based on $<$2.5th percentile) 3 left-side errors; allocentric asymmetry for incomplete apples (based on $<$2.5th percentile) 1 left-side errors. The cut-off for total numbers of target omissions (i.e., accuracy score) was 40/50 (based on $<$2.5th percentile).

In the majority of previous reports (and also in our study), patients showing neglect predominantly suffered from unilateral deficits on the left side following right brain damage. Therefore we restricted our analyses to left unilateral neglect (i.e., we used left asymmetry scores as main covariates of interest, but right asymmetry scores were also included as separate covariates in all statistical models). The behavioural scores used in the neuroimaging analyses were classified based on cut-offs drawn from the BUCS (i.e., for the covariates used in the statistical models patients missing fewer than 10 full apples and with fewer than 4 left errors on the left of the page or fewer than 3 right errors on the right of the page were assigned a score of 0 for left or right egocentric neglect, respectively, while patients with fewer than 2 false alarms to incomplete apples with a gap on the left or right were assigned a score of 0 for left or right allocentric neglect accordingly). Furthermore, in order to account for variation in overall performance affected by general motor and attentional deficits we took the asymmetry score for full apples and divided it by the total number of full apples missed. The normalized scores are shown in Appendix C.

Neuroimaging assessment

Patients and controls were scanned at the Birmingham University Imaging Centre (BUIC) on a 3T Philips Achieva MRI system with 8-channel phased array SENSE head coil. The anatomical scan was acquired using a sagittal T1-weighted sequence (sagittal orientation, echo time/time to repetition, TE/TR = 3.8/8.4 ms, voxel size $1 \times 1 \times 1$ mm^3). In addition, out of the 41 patients, 19 (including 1 patient with carbon monoxide poisoning) were scanned using a diffusion tensor imaging (DTI) sequence employing echo planar imaging (64 slices with isotropic $2 \times 2 \times 2$-mm^3 voxels, TR = 6,170 ms, TE = 78 ms). DTI was acquired in 61 gradient directions with a b value of 1,500 s/mm^2, and 1 volume was acquired with no diffusion weighting ($b = 0$ image).

Image analyses: T1 data

Image preprocessing. All T1 scans (both from patients and from controls) were first converted and reoriented using MRICro (Chris Rorden, University of South Carolina, Columbia, SC, USA). Preprocessing was done in SPM5 (Statistical Parametric Mapping; Friston, Ashburner, Kiebel, Nichols, & Penny, 2007, Welcome Department of Cognitive Neurology, London, UK). The earlier versions of SPM struggled with normalizing and segmenting brains containing large lesions (e.g., Stamatakis & Tyler, 2005) but here we applied the advanced unified-segment procedure as implemented in SPM5. The brain scans were transformed into the standard MNI (Montreal Neurological Institute) space using the

unified-segmentation procedure (Ashburner & Friston, 2005), which has been shown to be optimal for spatial normalization of lesioned brains (Crinion et al., 2007). The unified-segmentation procedure involves tissue classification based on the signal intensity in each voxel and on a priori knowledge of the expected localization of grey matter (GM), white matter (WM), and cerebrospinal fluid (CSF) in the brain and an extra class to account for other sources of signal variability; the tissues are iteratively segmented and warped onto standard space. The outputs of this procedure are three classified tissue maps representing the probability that a given voxel "belongs" to a specific tissue class. Note that the segmented images represent the likelihood of each voxel being the classified tissue based on the intensity in the original image; for example, an abnormal GM tissue would be presented by a lower intensity/probability value than normal. The lesioned brain tissue (e.g., that affected by stroke) is typically mapped with reduced likelihood of representing either grey or white matter due to the change in signal intensities caused by brain damage. In the current study we tested only chronic patients, and thus in the majority of cases the region of the damaged tissue was "replaced"/ "filled" by CSF (as shown in Appendix B, Figure B1, A). In addition, to avoid misclassification of abnormal tissue as normal, the number of Gaussians per class was restricted to 1 for both GM and WM. We visually inspected each of the segmented scans to assess whether the segmentation and normalization were successful (for an example see Appendix B, Figure B1, A). Finally, the segmented images were smoothed with a 12-mm FWHM (full width at half maximum) Gaussian filter to accommodate the assumption of random field theory used in the statistical analysis (Worsley, 2003). The choice of 12-mm FWHM instead of default 8 mm was based on previous recommendations for single-case comparison studies (Salmond et al., 2002). The preprocessed GM and WM images were further used in the analyses to determine voxel-by-voxel relationships between brain damage and the two neglect scores (see below).

Voxel-based morphometry (VBM). Scans from 38 patients (3 patients with carbon monoxide poisoning were excluded from the final analyses; see Appendix A for details), segmented into individual WM and GM maps (see above for the preprocessing protocol), were used in a further statistical analysis with SPM5, to assess the relationship between WM and GM damage and neglect scores on voxel-by-voxel basis. We used parametric statistics within the framework of general linear model (Ashburner & Friston, 2000), and the analyses for WM and GM were carried out separately. In each statistical model we included the scores for left allocentric and left egocentric errors (both extracted from the Apple Cancellation Task, see above). This ensured that we could control and formally test common and dissociated neuronal substrates that contribute to these two types of neglect. Additionally, in the statistical model age, handedness and gender as well as scores for right allocentric and right egocentric errors were included as covariates of no interest. The inclusion of right deficit scores was done to avoid biasing the results based on a priori assumptions: For example, analyses excluding patients with left deficits limit inferences about any potential contributions of particular brain regions to both left and right deficits. Note that all analyses included neuroimaging data from left- and right-hemisphere-lesioned patients as well as from patients with bilateral lesions. Dissociating left allocentric from left egocentric neglect was achieved by using exclusive masking—that is, testing for a change in voxel intensity that correlated with allocentric ($p < .001$, uncorrected) but not with egocentric neglect ($p > .05$, uncorrected) and vice versa. Common mechanisms were tested using conjunction analyses (Nichols, Brett, Andersson, Wager, & Poline, 2005) to highlight changes in voxel intensity that correlated with both egocentric and allocentric neglect at $p < .005$ uncorrected. To reduce the likelihood of Type 1 errors, we report only clusters that are larger than 100 mm^3 (>50 voxels). Results are reported at the clusters level corrected for multiple comparisons ($p < .05$, familywise error, FWE, corrected), unless stated otherwise. The anatomical localization of the lesion sites was

based on the Duvernoy human brain atlas (Duvernoy, Cabanis, & Vannson, 1991) and the *Brain Atlas* by Woolsey et al. (Woolsey, Hanaway, & Gado, 2008). The brain coordinates are presented in the standardized MNI space.

Lesion reconstruction and nonparametric lesion mapping. In addition to lesion analysis based on a general linear model (Ashburner & Friston, 2000), we also carried out voxel-based lesion symptoms mapping (VLSM) using binary lesion maps and nonparametric statistics (Rorden, Karnath, & Bonilha, 2007). Tissue abnormalities (lesions) were first reconstructed using a voxel-based analysis with SPM5 by comparing each patient's segmented GM and segmented WM to the segmented GM and segmented WM of the 73 healthy controls. Note that in order to objectively delineate brain abnormalities, medical condition (patient, control) was the independent variable while age and gender were modelled as covariates. GM and WM abnormalities were defined as changes of patient from controls that exceeded the stringent threshold of $p < .05$ corrected for familywise error with an extended cluster threshold of at least 100 voxels (larger than $\sim$200 mm^3). The results were verified against each patient's T1 scans (as well as T2 or fluid-attenuated inversion recovery, FLAIR, images if available), and binary maps of GM and WM lesions were created for the next step of the analysis (see example in Appendix B, Figure B1, B and C]). The nonparametric lesion symptom mapping was performed using non-parametric mapping software (NPM; Rorden, Karnath, & Bonilha, 2007) (Chris Rorden, University of South Carolina, Columbia, SC, USA). We used the Brunner–Munzel test (Rorden et al., 2007) to determine the relationship between lesion location and neglect scores, separately for GM and WM maps. In the statistical model both Apple Cancellation Task scores (i.e., left allocentric and left egocentric errors) were included as covariates in order to separate the neuroanatomy of the two symptom patterns. In the same manner to the VBM analyses, the statistical models included age, handedness, and gender as well as scores for right allocentric and right egocentric errors. Results were considered significant at $p < .05$, FDR (false discovery rate) corrected. The anatomical localization of the lesion sites was based on the Duvernoy human brain atlas (Duvernoy et al., 1991) and the *Brain Atlas* by Woolsey et al. (Woolsey et al., 2008).

Image analyses: DTI data

Data processing. All DTI data sets were first converted using MRIcron (Chris Rorden, University of South Carolina, Columbia, SC, USA) and were then analysed using FMRIB Software Library (FSL; Smith et al., 2004, Oxford, UK). First, we used Eddy Current Correction tool to align all volumes (61 images encoding diffusion strength in all different directions and 1 image with no diffusion weighting, i.e., b0 volume). Eddy Current Correction, as implemented in FSL, corrects for gradient coil eddy currents distortions as well as for simple head motions using affine registration to a reference volume (b0 volume). Next, the fractional anisotropy (FA) maps were created using DTIFit within the FSL FDT toolbox (Smith et al., 2004). Subsequently, colour-coded orientation maps were generated, and the fibre orientation was assumed based on the eigenvector associated with the largest eigenvalue (Basser, Mattiello, & LeBihan, 1994). On the colour-coded orientation maps, red, green, and blue colours were assigned to the left–right, anterior–posterior, and superior–inferior orientations accordingly (Pajevic & Pierpaoli, 1999). The anatomical localization of specific white matter pathways was based on the *MRI Atlas of Human White Matter* by Mori (2005).

Voxel-wise analysis. The analysis of FA maps was carried out with SPM5. We used b0 volume to determine normalization parameters for the FA maps. First, for each participant all images (b0 volume and FA map) were realigned. Next, b0 volumes of all participants were normalized to the standard T2 template using linear transformations (Friston et al., 1995) based on previously published procedure (Salmond et al., 2006; Thomas et al., 2009). Subsequently FA maps

were normalized to a standard space based on the parameters from the processing of b0 volume. In order to restrict the analysis to white matter and to ensure that no results were caused by the close vicinity of grey matter, we created binary white-matter-specific mask in MNI space using the WFU Pick atlas toolbox in conjunction with SPM5 (Maldjian, Laurienti, Kraft, & Burdette, 2003). This mask was applied to all individual normalized FA maps prior to smoothing of the images. The smoothing was done with 8-mm FWHM Gaussian filter in order to improve the signal-to-noise ratio and to decrease between-subject variability. Finally, a voxel-wise analysis was carried out to investigate the relationship between the decreased anisotropy and neglect scores. We used an identical model, statistical tests, and threshold to those used in the analysis of the segmented WM data from the T1 images (see above). Results are reported at the cluster level corrected for multiple comparisons ($p < .05$, FWE corrected), unless stated otherwise. The anatomical localization of damage within specific white matter pathways was based on the *MRI Atlas of Human White Matter* by Mori (2005).

Results

Figure 1 shows the behavioural performance of all patients on the Apple Cancellation Task (for full neuropsychological data of the patient group see Appendix A). Out of the 41 tested patients, 11 showed left and 2 right allocentric neglect, and 8 patients showed left and 2 right egocentric neglect, assessed relative to control performance. Six patients showed both left egocentric and allocentric neglect, though the severity of impairment varied—with 3 patients having predominantly left egocentric neglect and 3 equal impairments for both types of deficit. One patient showed left allocentric and right egocentric neglect, with equal degrees of severity (see also Riddoch, Humphreys, Luckhurst, Burroughs, & Bateman, 1995). Similarly to previous reports, patients in our study predominantly suffered from unilateral left deficits (Figure 1, B and C). Therefore we restricted further neuroimaging analyses to left unilateral neglect but we used both left and right asymmetry scores for allocentric and egocentric neglect in all statistical models (see Method for details). As some brain regions may contribute to both left and right deficits, this approach was used to avoid biasing the results based on a priori assumptions (e.g., preselecting patients based on their anatomical lesions or behavioural scores).

Note that in the following analyses we used continuous scores for both types of neglect. This increased the sensitivity of these measures by accounting for the severity of the symptoms and not just for their categorical presence. Using these continuous scores we could test for correlations between the severity of allocentric and egocentric neglect. Interestingly, there was no significant correlation between these two types of neglect (Figure 1E; $r = .145$ at $p = .231$), supporting a dissociative account of the syndrome (see also Hillis et al., 2005).

Grey matter: Allocentric versus egocentric neglect

We used two different statistical methods (parametric and nonparametric) to covary out allocentric and egocentric components of visual neglect in our lesion analyses, providing a novel comparison of the two approaches. Specifically, using a VBM approach we found that lesions in the right hemisphere within angular, middle temporal (partly extending into inferior temporal), middle occipital gyri, and the posterior superior temporal sulcus resulted in left allocentric neglect (Figure 2, A and D; see Table 1 for peak MNI coordinates). In contrast, damage within the right middle frontal, postcentral, supramarginal, anterior, and central superior temporal gyri and the insula (Figure 2, B and D; see Table 1 for peak MNI coordinates) was associated with egocentric errors on the left side of the page. In addition, we found associations between egocentric but not allocentric neglect and lesioned voxels within subcortical structures (Figure 2B) including the pulvinar and basal ganglia.

Importantly, the VBM approach also allowed us to test for substrates that are common for both types of neglect. The VBM conjunction analysis revealed that damage within right anterior

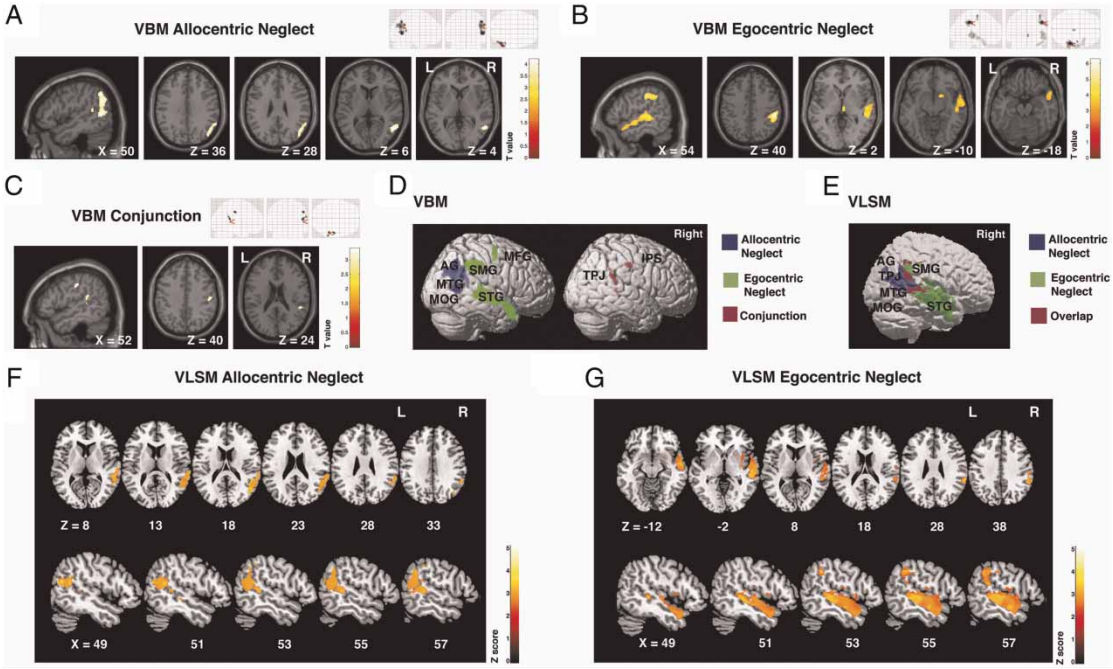

Figure 2. *Voxel-wise statistical analysis of grey matter damage: allocentric versus egocentric neglect. VBM = voxel-based morphometry; VLSM = voxel-based lesion symptoms mapping. Both VBM (A, B) and VLSM (F, G) indicated a striking anterior–posterior dissociation between grey matter substrates of left allocentric and left egocentric neglect. (C) VBM-based conjunction analysis also revealed that damage within right IPS and right TPJ was associated with both left allocentric and left egocentric errors. (D) VBM and (E) VLSM results indicating both distinctions and commonalities between the grey matter substrates of left allocentric and left egocentric neglect displayed on brain render. Please note that in A, B, and C the lesioned areas are coloured according to the significance level in the VBM analysis, where brighter colour means higher* t*-value. In F and G statistical maps are displayed after applying a statistical threshold of* $p < .05$*, FDR (false discovery rate) corrected, and are coloured according to the significance level where brighter colour means higher* z *score. MNI (Montreal Neurological Institute) coordinates of transverse and sagittal sections are given. AG, angular gyrus; IPS, intraparietal sulcus; MOG, middle occipital gyrus; MTG, middle temporal gyrus; SMG, supramarginal gyrus; STG, superior temporal gyrus; TPJ, temporal-parietal junction.*

intraparietal sulcus (IPS) and right temporo-parietal junction (TPJ) was associated with both left allocentric and left egocentric errors on the Apple Cancellation Task (Figure 2, C and D; see Table 1 for peak MNI coordinates).

Similarly to the VBM results, our VLSM analysis demonstrated that lesions in the right hemisphere within the angular gyrus ($z = 3.49$; peak MNI coordinates: 56, −49, 32), the middle temporal gyrus extending into superior temporal sulcus ($z = 3.89$; peak MNI coordinates: 50, −48, 18), and the middle occipital gyrus ($z = 3.07$; peak MNI coordinates: 40, −77, 32) resulted in left allocentric neglect (Figure 2, E and F). Furthermore, the VLSM analysis linked damage within the right supramarginal gyrus ($z = 3.62$; peak MNI coordinates: 54, −42, 37), the right anterior and central superior temporal gyrus ($z = 3.43$; peak MNI coordinates: 54, −27, 2), and the right insula ($z = 2.72$; MNI peak coordinates: 39, −15, 1) with egocentric errors on the left side of the page (Figure 2, E and G). In addition, we found associations between egocentric but not allocentric neglect and lesioned voxels within the right basal ganglia ($z = 2.89$; peak MNI coordinates: 20, 9, −10). Finally, we found that, similarly to the VBM conjunction analysis, the VLSM statistical maps of lesion distribution in allocentric and egocentric neglect overlapped within the TPJ, within the posterior IPS, and also within the border between the middle and superior temporal gyri (Figure 2E).

Table 1. *Grey matter substrates: Left allocentric versus left egocentric neglect: Results from VBM analysis*

	Cluster level		*Voxel level*	*Coordinates*			
Contrast	p_{corr}	*Size*	*z-score*	*X*	*Y*	*Z*	*Brain structure*
Allocentric errors	.000	830	3.73	**54**	**−58**	**6**	right MTG/ITG[a] and MOG
($p < .001$ uncorr.)			3.60	50	−58	44	right posterior STS
			3.57	50	−62	30	right AG
Egocentric errors	.000	596	5.04	**52**	**−32**	**40**	right SMG
($p < .001$ uncorr.)	.000	980	3.71	**48**	**−24**	**−8**	right STG
			3.68	54	−30	2	right insula
	.034	80	4.18	**44**	**−8**	**62**	right MFG
	.140	58	4.03	**4**	**−22**	**−2**	right pulvinar
	.881	51	3.50	**16**	**8**	**−10**	right basal ganglia
Conjunction	.924	73	3.11	**50**	**−38**	**18**	right TPJ
($p < .005$ uncorr.)	1.000	46	3.07	**50**	**−22**	**40**	right IPS

Note: VBM = voxel-based morphometry; AG = angular gyrus; IPS = intraparietal sulcus; ITG = inferior temporal gyrus; MOG = middle occipital gyrus; MTG = middle temporal gyrus; SMG = supramarginal gyrus; STG = superior temporal gyrus; STS = superior temporal sulcus; TPJ = temporal-parietal junction. MFG = middle frontal gyrus. Bold denotes maximum peak, the coordinates not in bold denote local maxima.

[a]Lesion within middle temporal gyrus partly extending into inferior temporal gyrus.

In summary, our VBM analyses converge with VLSM in demonstrating both common and distinct sets of grey matter lesions linked to the two symptoms of neglect. Importantly, both VBM, based on general linear modelling, and VLSM demonstrated a striking dissociation between egocentric and allocentric neglect: Allocentric neglect was reliably associated with more posterior grey matter damage, while egocentric neglect was linked to more anterior grey matter damage as well as to lesions within subcortical structures.

White matter: Allocentric versus egocentric neglect

Similar to our assessments of grey matter damage we used converging statistical and imaging methods to analyse white matter damage, covarying out allocentric and egocentric components of visual neglect (Figures 3 and 4, Table 2). Note that, by using T1-contrast images alone, it is difficult to accurately depict the location of damaged voxels within specific white matter tracts. Therefore, one reason for using DTI was to provide a more precise localization of the white matter lesions within a specific pathway. This enabled us to generate qualitative evaluations of colour-coded orientation maps, generated directly based on diffusion tensor vector data that visualize specific pathways (Figure 4, A and C). The results of the statistical analyses (below) were then verified against the individual colour-coded orientation maps.

The neuronal correlates of allocentric and egocentric neglect based on VBM analyses of segmented white matter indicated that the two neglect symptoms were linked to damage within common white matter pathways (Figure 3, A and B; see Table 1 for peak MNI coordinates). Similarly, the nonparametric mapping (VLSM) of white matter lesions of neglect symptoms also showed a clear commonality between the white matter substrates of allocentric and egocentric neglect (Figure 3, D and E). Specifically, white matter lesions consistent with damage within long association and projection pathways including the right superior longitudinal fasciculus (SLF) and superior fronto-occipital fasciculus (SFO; allocentric—$z = 3.89$, peak MNI coordinates: 24, 0, 36, and $z = 4.03$, peak MNI coordinates 35, −39, 27; egocentric—$z = 3.89$, peak MNI coordinates: 22, −32, 49), the right inferior fronto-occipital fasciculus (IFOF) and inferior longitudinal fasciculus (ILF; allocentric—$z = 3.84$, peak MNI coordinates: 35, −48, 11;

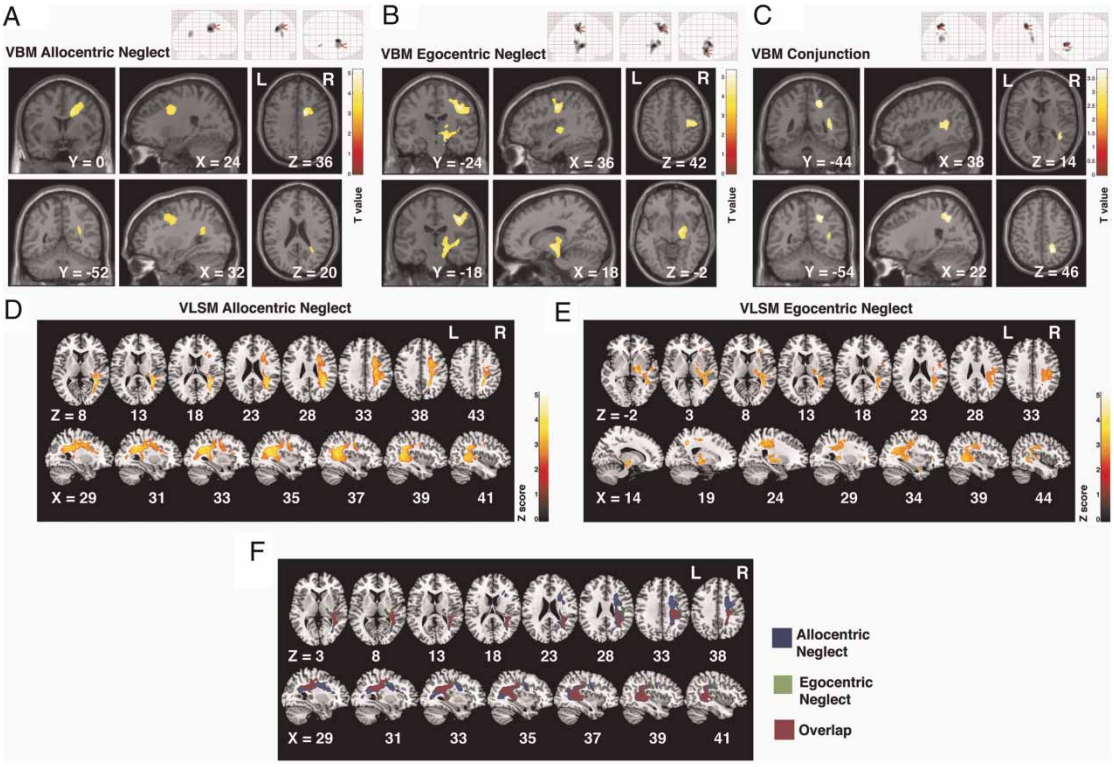

Figure 3. *Voxel-wise statistical analysis of white matter damage: allocentric versus egocentric neglect. VBM (voxel-based morphometry) results showing voxels corresponding to white matter damage in (A) left allocentric, (B) left egocentric, and (C) both forms of neglect (conjunction analysis). Please note that in A, B, and C the lesioned areas are coloured according to the significance level in the VBM analysis, where brighter colour means higher* t*-value. The results of nonparametric analysis of white matter lesions (VLSM, voxel-based lesion symptoms mapping) in (D) left allocentric, (E) left egocentric neglect. Please note that in D and E statistical maps are displayed after applying a statistical threshold of* $p < .05$*, FDR (false discovery rate) corrected, and are coloured according to the significance level, where brighter colour means higher* z *score. (F) VLSM statistical maps of lesion distribution in allocentric and egocentric neglect showed significant overlap within the same white matter pathways. MNI (Montreal Neurological Institute) coordinates of coronal, sagittal, and transverse sections are given.*

egocentric—$z = 3.72$, peak MNI coordinates: 36, −61, 21), and right thalamic radiation and right corona radiata (allocentric—z score = 3.71, peak MNI coordinates: 24, −8, 40; egocentric—z score = 3.55, peak MNI coordinates: 35, −26, 3), were associated with both sets of symptoms.

To further investigate the common white matter lesions across the two neglect symptoms, we used conjunction analysis. VBM-based conjunction analysis of segmented white matter lesions from the T1 images showed that damage within regions that seem to be a part of the right posterior SLF, posterior IFOF, posterior ILF, superior corona radiata, and superior and posterior thalamic radiations was associated with both allocentric and egocentric neglect (Figure 3C; Table 2). Furthermore, we found that, similarly to the VBM conjunction analysis, the VLSM statistical maps of the lesion distribution in allocentric and egocentric neglect showed significant overlap within the same white matter pathways (Figure 3F).

Finally, the conjunction analysis based on the DTI data from a subset of patients showed a decrease in fractional anisotropy in the regions of right white matter that include the following pathways: ILF, IFOF, SLF, SFO, superior and posterior thalamic radiation, and anterior and superior corona radiata (Figure 4E; Table 3).

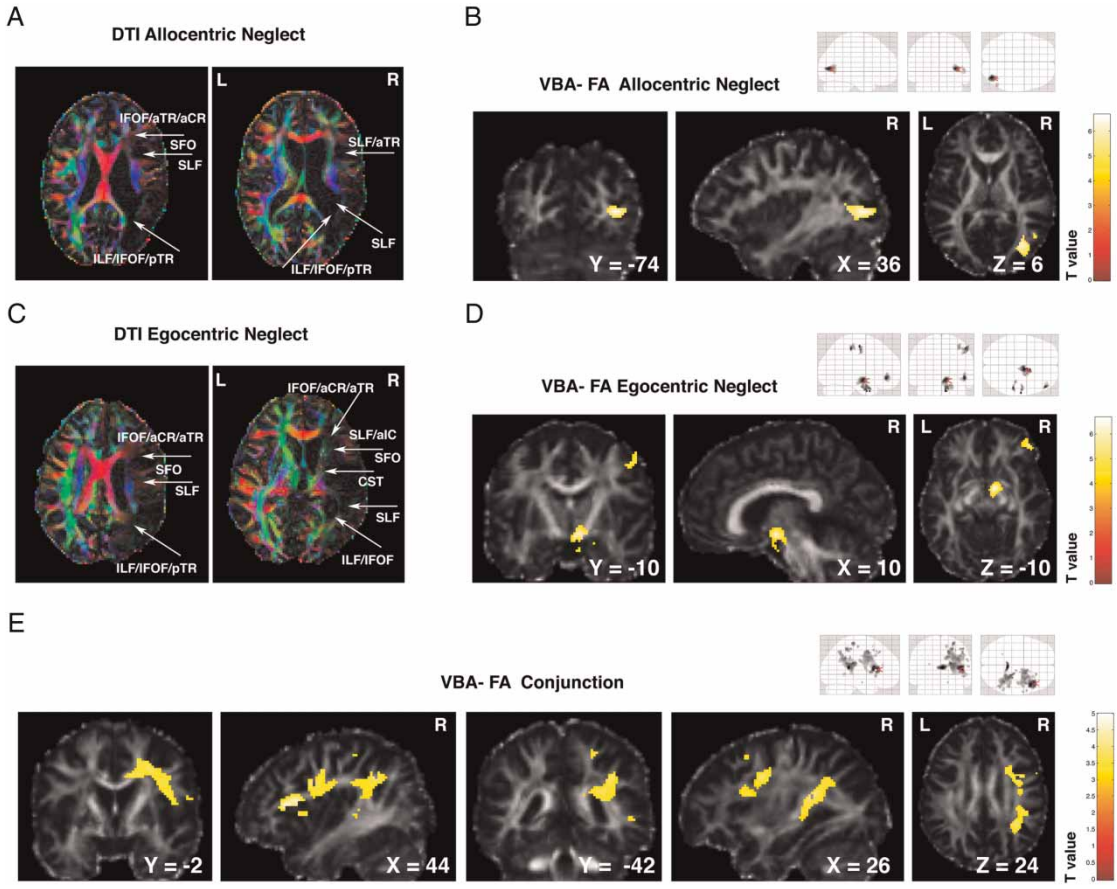

Figure 4. *Changes in fractional anisotropy: allocentric versus egocentric neglect. Examples of colour-coded orientation maps showing damage within specific white matter pathways in patient with (A) left allocentric and (C) left egocentric neglect. Voxel-wise statistical analysis of white matter integrity based on FA (fractional anisotropy) in (B) left allocentric, (D) left egocentric, and (E) both forms of neglect (conjunction analysis). Please note that similarly to VBM (voxel-based morphometry) and VLSM (voxel-based lesion symptoms mapping) analyses of white matter lesions (Figure 3) the damaged areas in both forms of neglect were located within the same white matter pathways. MNI (Montreal Neurological Institute) coordinates of coronal, sagittal, and transverse sections are given. VBA = voxel-based analysis; DTI = diffusion tensor imaging. aCR, anterior corona radiata; aIC, anterior limb of internal capsule; aTR, anterior thalamic radiation; CST, corticospinal tract; IFOF, inferior fronto-occipital fasciculus; ILF, inferior longitudinal fasciculus; pTR, posterior thalamic radiation; SFO, superior fronto-occipital fasciculus; SLF, superior longitudinal fasciculus.*

These results were strikingly similar to the findings derived from the segmented white matter using T1 images. Note, however, that the DTI-based analyses showed higher sensitivity to white matter damage than did the T1 analyses, despite being based on a smaller number of patients. This suggests that DTI indices such as fractional anisotropy (FA) may be a more sensitive way in measuring changes in white matter integrity that are associated with abnormal cognitive function—that is, DTI allows to identification of even small changes in white matter integrity outside lesion sites detectable by high-resolution T1-weighted imaging. The T1- and DTI-based conjunction analyses did not converge with respect to differential white matter damage within the frontal lobe. The cause of these discrepancies is unclear—it may be due to the differences in imaging methods itself, or to differences between the subset of patients with acquired DTI compared to the whole group.

Table 2. *White matter substrates: Left allocentric versus left egocentric neglect: Results from VBM analysis*

	Cluster level		*Voxel level*	*Coordinates*			
Contrast	p_{corr}	$Size_c$	*z-score*	*X*	*Y*	*Z*	*Brain structure*
Allocentric errors ($p < .001$ uncorr.)	.000	691	4.39	**16**	**0**	**36**	right ant. SFO and SLF
			3.50	32	0	42	right sup. CR and TR
			3.48	28	10	42	
	.094	76	3.50	**32**	**−52**	**20**	right post. ILF and IFOF
Egocentric errors ($p < .001$ uncorr.)	.000	694	4.50	**42**	**−18**	**42**	right SFO and SLF, right sup. CR and TR, right post. IC and CST
			4.01	34	−14	52	right post. ILF and IFOF
			3.87	48	−24	48	right CST, right sup. TR, right post. IC
	.000	949	4.45	**22**	**−8**	**−2**	
			3.95	36	−24	6	
			3.83	18	−18	−10	
Conjunction ($p < .005$ uncorr.)	.00	266	3.44	**22**	**−54**	**46**	right sup. SLF, CR, and TR
			3.27	20	−44	50	
	.014	177	3.19	**38**	**−48**	**14**	right post. SLF, ILF, IFOF, and TR

Note: The location of white matter lesions suggests damage to specific white matter pathways as listed in the right-hand column. VBM = voxel-based morphometry; ant = anterior; post = posterior; sup = superior; CR = corona radiata; CST = corticospinal tract; IC = internal capsule; IFOF = inferior fronto-occipital fasciculus; ILF = inferior longitudinal fasciculus; SFO = superior fronto-occipital fasciculus; SLF = superior longitudinal fasciculus; TR = thalamic radiation. Bold denotes maximum peak, the coordinates not in bold denote local maxima.

Importantly, the results from VBM, VLSM, and DTI analyses also indicated some dissociations in white matter damage between the two types of neglect. Both T1-based approaches suggest that egocentric neglect involves damage to white matter surrounding the thalamic and basal ganglia nuclei (Figure 3, B and E, Figure 4D). This extends the grey matter results that suggest involvement of pulvinar and basal ganglia in egocentric neglect. Moreover, the DTI and VLSM results indicate that allocentric neglect is associated with damage to more posterior white matter in superior parts of the occipital cortex (Figure 3F and Figure 4B), which again extends the grey matter results suggesting that overall allocentric neglect is associated with more posterior lesions.

In summary, both of the T1-based approaches we used (VBM and VLSM) converge with the DTI-based analyses in demonstrating common white matter lesions across the two neglect symptoms. In particular, lesions within white matter regions that suggested damage within long association pathways, including the ILF, the IFOF, and the SLF, were linked to both types of deficit.

Discussion

Cortical lesions

Here, we examined how damage to grey matter and subcortical white matter tracts affect two separate neglect symptoms: egocentric (misses on the left side of the page) and allocentric errors (false alarms to distractors with a left-side gap) in a group of chronic neurological patients. This is in contrast to prior studies, which have examined the neuroanatomical bases of acute visual neglect without differentiating the grey and white matter substrates. We demonstrated both common and distinct sets of lesions linked to the two symptoms of neglect. Most strikingly, we found that there were contrasting regions of cortical damage linked to egocentric and allocentric errors, with allocentric errors associated with more posterior damage (posterior superior temporal sulcus, and angular, middle temporal/inferior temporal, and

Table 3. *White matter substrates: Left allocentric versus left egocentric neglect: Results from VBA–FA analysis*

	Cluster level		*Voxel level*	*Coordinates*			
Contrast	p_{corr}	*Size*	*z-score*	*X*	*Y*	*Z*	*Brain structure*
Allocentric errors	.000	212	3.96	**36**	**−74**	**6**	right post. ILF, IFOF, and CR
($p < .001$ uncorr.)			3.40	38	−64	6	right post. SLF and ILF
	.000	56	3.28	**56**	**−64**	**4**	
Egocentric errors	.000	373	4.23	**10**	**−4**	**−10**	right ant. and sup. TR
($p < .001$ uncorr.)			4.13	8	0	−28	right IC and CST
			4.12	10	8	32	
	.000	108	4.19	**48**	**42**	**−6**	right ant. IFOF
	.000	124	4.17	**50**	**−30**	**52**	right ant. SLF and CR
			3.82	54	−10	50	right sup. TR and CR
			3.47	36	−24	54	
Conjunction	.000	1,245	3.52	**44**	**16**	**16**	right ant. SFO, SLF, IFOF, and CR
($p < .005$ uncorr.)			3.44	16	4	48	
			3.17	40	24	12	right sup. and post. TR, right post. SLF, ILF, and IFOF
	.001	966	3.59	**22**	**−28**	**22**	
			3.26	2	−36	14	right sup. CR and TR
			3.14	38	−46	34	
	.995	65	3.11	**24**	**−42**	**52**	

Note: The location of white matter lesions suggests damage to specific white matter pathways as listed in the right-hand column. VBA = voxel-based analysis; FA = fractional anisotropy; ant = anterior; post = posterior; sup = superior; CR = corona radiata; CST = corticospinal tract; IC = internal capsule; IFOF = inferior fronto-occipital fasciculus; ILF = inferior longitudinal fasciculus; SFO = superior fronto-occipital fasciculus; SLF = superior longitudinal fasciculus; TR = thalamic radiation. Bold denotes maximum peak, the coordinates not in bold denote local maxima.

middle occipital gyri) than egocentric errors (middle frontal, postcentral, supramarginal, and superior temporal gyri as well as the insula). These distinct sites of cortical damage incorporate brain regions contrasted in prior studies of the lesion–symptom mapping in neglect. For example, the analyses reported by Karnath and colleagues (Karnath et al., 2004a; Karnath et al., 2002) highlight the association between neglect and relatively anterior cortical regions including the middle superior temporal gyrus (mSTG), the insula, and the pre- and postcentral gyri as well as subcortical structures such as putamen, caudate, and pulvinar. In our analysis, egocentric neglect was linked to lesions to STG, the supramarginal gyrus, the postcentral gyrus, middle frontal gyrus, and insula as well as lesions within basal ganglia and pulvinar. Verdon et al. (2010) also reported that deficits in visuomotor exploration of egocentric space was associated with relatively anterior lesions, including damage to dorsolateral prefrontal cortex.

In contrast to these data highlighting relatively anterior lesions, the analyses reported by Mort et al. (2003) stressed that damage to the angular gyrus and the medial temporal lobe/parahippocampus was linked to neglect. We found more specifically that damage to these regions was associated with allocentric neglect. Our data indicate that discrepancies between prior studies may reflect the heterogeneous nature of the neglect symptoms. Karnath and colleagues (Karnath et al., 2004a; Karnath et al., 2002) have tended to measure neglect using tasks that require exploration through multiple separate objects, similar to our measure of egocentric neglect. In contrast, Mort et al. (2003) employed, as a part of cognitive assessment, line bisection to measure

neglect, a task that may be performed by spreading attention across each target line—this would make the task similar to our measure of allocentric neglect (though see Verdon et al., 2010, for a different view). In addition, our results are in line with the findings of Rorden et al. (2006) and Verdon et al. (2010), who reported that poor performance on line bisection was associated with posterior brain lesions additional to those found in patients showing neglect only on cancellation and exploration tasks (Rorden et al., 2006; Verdon et al., 2010). Also like Verdon et al. (2010) we link spatial impairments in attending in allocentric space to deficits impinging on medial and inferior occipital-temporal cortex. In sum, we suggest that different aspects of neglect are associated with these contrasting lesion sites, with the variations in neglect contributing to the discrepancies in previous findings. Furthermore, our combined analyses of the grey and white matter lesions provide a novel contrast between symptom-specific grey matter damage and symptom-general white matter damage.

Subcortical white matter lesions

In addition to the distinct sites of grey matter damage, we found common white matter lesions across the two neglect symptoms. In particular, lesions within white matter regions suggesting damage within long association pathways, including the ILF, the IFOF, and the SLF, were linked to both measures. These white matter structures may be critical for aligning interactions between neural regions that compete in different ways to select target objects—for example, connecting between maps that compete to represent different visual features in particular locations, in relation to, respectively, the participant's body and the objects they are part of (Heinke & Humphreys, 2003). As a consequence, damage to the connecting white matter pathways leads to both egocentric and allocentric neglect. Doricchi and Bartolomeo (Bartolomeo et al., 2007; Doricchi, Thiebaut de Schotten, Tomaiuolo, & Bartolomeo, 2008; Doricchi & Tomaiuolo, 2003) used data on white matter deficits associated with neglect to propose that neglect should be considered as a disconnection syndrome. However, while cortical and subcortical connections are undoubtedly damaged in the disorder, our results indicate that a disconnection account would miss the critical distinction that exists between allocentric and egocentric forms of deficit, which are associated with distinct cortical sites (see also Verdon et al., 2010). Lesions to white matter tracts will mean that the different spatial representations may fail to be transmitted to response systems, but the cortical substrates of the representations also appear critical.

In a recent study, Karnath et al. examined grey matter versus white matter predictors of spatial neglect (Karnath, Rorden, & Ticini, 2009) based on a reanalysis of previous data from this group (Karnath et al., 2004a). Karnath et al. (2009) combined a voxel-wise lesion–symptom mapping analysis of manually drawn lesions from either MRI or computed tomography (CT) scans collected at an acute stage of stroke with a probabilistic white matter atlas (the Jülich atlas). The results showed that overall grey matter lesions, particularly within superior temporal, inferior parietal, inferior frontal, and insular cortices and subcortical structures (such as the caudate and putamen), were stronger predictors of spatial neglect than were white matter lesions within the SLF, IFOF, and SFO. In contrast to these findings, our VBM analyses suggest that both grey and white matter lesions are strongly associated with neglect symptoms. The stronger association between white matter damage and neglect symptoms in our study may be explained by a greater sensitivity of our analyses, including DTI and a secondary white matter degeneration of axonal structures present in chronic but not acute patients (see Footnote 2).

Functional accounts of neglect

These data, plus also those emerging from a number of recent neuroimaging studies (Hillis et al., 2005; Marsh & Hillis, 2008; Rorden et al., 2006; Verdon et al., 2010), strongly indicate that visual neglect should not be considered to be a unitary syndrome; rather there can be a number of functionally distinct deficits, subserved by different brain regions, which can lead to contrasting spatial biases in visual selection. In

this case, the neurological data constrain functional interpretations of the deficit.

We can consider at least two functional accounts of these results. One is that the contrasting cortical regions support distinct spatial representations of the visual world (Humphreys, 1998). Representations of multiple separate objects are required to support spatial exploration across the page in cancellation tasks, and asymmetrical lesions of these representations may result in egocentric neglect. This would link the supramarginal and postcentral gyri and superior temporal gyrus to representing the locations of multiple separate objects with respect to the patient (a "between-object" spatial representation; Humphreys, 1998). In contrast, the angular gyrus, medial temporal lobe, and middle occipital gyrus are involved in representing the spatial locations within objects. An asymmetrical lesion to these representations will lead to allocentric (within-object) neglect.

Alternatively, these different neural regions may support the allocation of attention to the contrasting spatial representations held in other areas, or the regions may support processes that read in visual information (for egocentric neglect) or that read out information (for allocentric neglect) from neural networks involved in selecting between stimuli that compete for object recognition. In the computational model of Heinke and Humphreys (2003), for example, visual information is fed into a selection network where separate objects compete for entry into a focus of attention, which itself gates access to stored object knowledge. Selected objects are registered in a location map, which reflects the salience of stimuli in the visual field (selective attention for identification model, SAIM; Figure 5). Heinke and Humphreys demonstrated that damage affecting the visual information coming into one side of the competition network led to egocentric neglect, with there being poor recovery of stimuli on one side of retinally defined space. In contrast, damage affecting the output from the selection network coming into one side of the

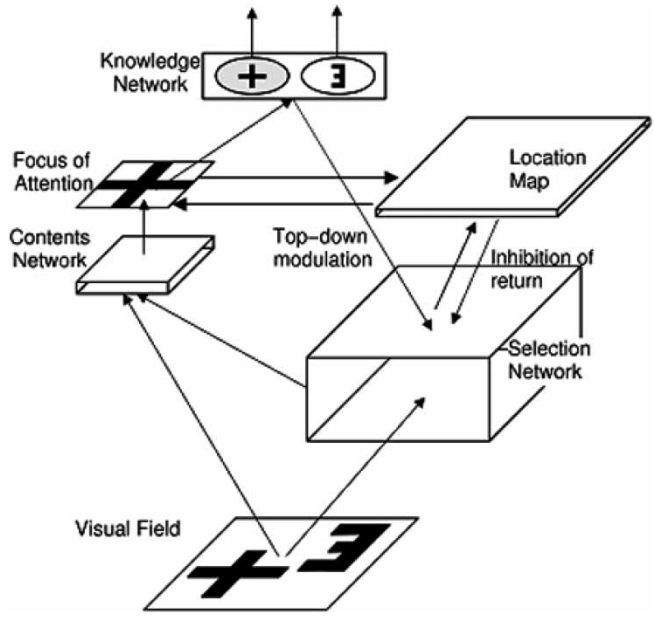

Figure 5. *The selective attention for identification model (SAIM) of visual selection. From "Attention, Spatial Representation, and Visual Neglect: Simulating Emergent Attention and Spatial Memory in the Selective Attention for Identification Model (SAIM)", by D. Heinke and G. W. Humphreys, 2003,* Psychological Review, 110, *p. 33. Copyright 2003 by the American Psychological Association. Adapted with permission of D. Heinke and G.W. Humphreys.*

focus led to allocentric neglect, with the contralesional parts of objects being neglected irrespective of their lateral position in the field. From the current data, input into the selection network would be mediated by regions including the supramarginal, the postcentral, and the superior temporal gyrus; access into the focus of attention would operate through the angular gyrus and more medial occipito-temporal cortex. Interestingly, in a recent model-based analysis of functional magnetic resonance imaging (fMRI) data from human search, Mavritsaki, Allen, and Humphreys (2010) have argued for an association between activity in a saliency map in their model and activation of the right temporo-parietal junction (TPJ) in humans. Spatially specific damage to the location map in SAIM would lead to poor representation of both whole stimuli on the contralesional side, and also contralesional parts of stimuli, if this location map feeds back activity to influence activation in the focus of attention and the selection network (see Mavritsaki, Heinke, Deco, & Humphreys, 2009). This would be consistent with our finding that the right TPJ is associated with both allo- and egocentric neglect.

Alongside the cortical deficits, SAIM may also be able to account for the data from damage to white matter tracts. One proposal stresses neuroanatomical proximity. For example, within the model there will be close "anatomical" overlap between the tracts that lead from the selection network and the focus of attention into the location map. As a consequence, damage to brain regions where those tracts link to the location map will generate both allocentric and egocentric neglect, since there will be problems in registering both objects on one side of egocentric space (connections from the selection network) and the elements on one side of each selected object (connections from the focus of attention). In addition, top-down projections from higher level recognition systems in the model (the knowledge network) carry information about both the location of the object and the locations of elements within objects. Consequently, damage to these projections may generate both profiles of neglect.

A somewhat different way to think about the functional deficits linked to our lesion analysis is that the impairments reflect unilateral problems in attending to local and global spatial representations. For example, the egocentric problems we have identified could be linked to poor attention to one side of a global spatial representation (the positions of the separate objects on the page), while allocentric deficits could stem from impaired attention to the contralesional side of local spatial representations (the locations of the gaps on each object). Arguments for a critical role for impairments in global spatial representations in the neglect syndrome have been made previously. Halligan and Marshall (1994) proposed that neglect emerges from two deficits—an ipsilesional bias in attention coupled to an impaired global spatial representation. These authors argued that, due to these combined problems, patients attend to local areas of space on the ipsilesional side and fail to reorient contralesionally. This proposal could account for the symptoms of egocentric neglect that we have reported, but not for the allocentric deficits in attending to parts within objects. In addition, poor attention to local spatial areas has tended to be associated with left hemisphere rather than right hemisphere damage (Delis, Robertson, & Balliet, 1983), whereas our data highlight a right hemisphere association with allocentric deficits. More detailed studies also suggest that allocentric deficits are unlikely to be fully accounted for in terms of unilateral impairments to local spatial representations. Consider the patient of Humphreys and Riddoch (1994), who presented with left allocentric (e.g., making errors on the left side of individual words) but right egocentric neglect (missing whole words on the right of the page). This patient continued to display the same allocentric problems when letters were expanded across the page so that a single word then covered the same area as sets of smaller, individual words in previous tests. Thus, the patient read the enlarged letters in areas on the right of the page where he had previously omitted whole words, but he made errors to letters on the left of the enlarged words in regions where previously he detected smaller

whole words. In such a case, the size of the spatial area covered by the stimuli seems less critical than whether the patient is attempting to scan from one independent object to another (where he had a deficit on the right side of space) or is assimilating all the elements together as part of a single perceptual object (where he had a deficit on the left side of space). Nevertheless, the argument about local and global representations is itself compatible with models such as SAIM. Within SAIM, competition within the selection network operates at a global level of spatial representation, between separate objects in the visual field. In contrast, the assimilation of elements into the focus of attention operates at a more local level of the individual selected object. The model provides a framework for understanding the inter-relation between global and then more local selection processes.

Our argument for posterior occipital-temporo-parietal sites being important for allocentric processing contradicts Vallar et al. (2003) and Medina et al. (2009), who associated allocentric neglect with ventral stream lesions and egocentric neglect with dorsal stream lesions. Partly this may reflect differences in test material, with some studies using items with clearer lexico-semantic representations than our figures, and these lexico-semantic stimuli may recruit more ventral cortex. Previously, Karnath (2001) proposed that the superior temporal cortex in humans, which receives inputs from both dorsal and ventral visual stream, should be considered as an interface between allocentric and egocentric visual attention systems. We found that lesions within superior temporal cortex were associated with both forms of neglect, though with there remaining an anterior–posterior subdivision consistent with the general anterior–posterior distinction between egocentric and allocentric deficits (posterior superior temporal sulcus, STS/allocentric; anterior and central superior temporal gyrus, STG/egocentric neglect). Nevertheless, our data fit with the superior temporal cortex being an important convergence region, bringing together different forms of spatial representation. Our results suggest, however, that the convergence is not simply from ventral and dorsal pathways but may include bringing together different spatial representations within a parieto-frontal network. We note too that Medina et al. (2009) found an association between damage within STG and egocentric neglect, while their previous study showed association between STG and allocentric neglect (Hillis et al., 2005). Our finer grained analysis suggests that both types of neglect can arise after damage to the superior temporal cortex, though differences may emerge when the lesion is sufficiently small to selectively affect more anterior or posterior sections.

Conclusions

We conclude that our data point to distinct cortical regions controlling attention (a) across space (using an egocentric frame of reference) and (b) within objects (using an allocentric frame of reference), along with common cortical regions and white matter pathways that support interactions across the different cortical regions. We suggest that egocentric codes computed in a fronto-parieto-temporal network and integrated with allocentric codes computed in a parieto-temporal-occipital network converge within IPS, TPJ, and superior temporal cortex and share common white matter pathways. These distinct regions can be linked to different functional modules within computational models of human visual selection.

Manuscript received 3 February 2010
Revised manuscript received 1 August 2010
Revised manuscript accepted 23 August 2010

REFERENCES

Ashburner, J., & Friston, K. J. (2000). Voxel-based morphometry—the methods. *NeuroImage*, *11*(6, Pt. 1), 805–821.

Ashburner, J., & Friston, K. J. (2005). Unified segmentation. *NeuroImage*, *26*(3), 839–851.

Bartolomeo, P., Thiebaut de Schotten, M., & Doricchi, F. (2007). Left unilateral neglect as a disconnection syndrome. *Cerebral Cortex*, *17*(11), 2479–2490.

Basser, P. J., Mattiello, J., & LeBihan, D. (1994). MR diffusion tensor spectroscopy and imaging. *Biophysical Journal*, *66*(1), 259–267.

Binder, J., Marshall, R., Lazar, R., Benjamin, J., & Mohr, J. P. (1992). Distinct syndromes of hemineglect. *Archives of Neurology*, *49*(11), 1187–1194.

Bird, C. M., Malhotra, P., Parton, A., Coulthard, E., Rushworth, M. F., & Husain, M. (2006). Visual neglect after right posterior cerebral artery infarction. *Journal of Neurology, Neurosurgery, and Psychiatry*, *77*(9), 1008–1012.

Crinion, J., Ashburner, J., Leff, A., Brett, M., Price, C., & Friston, K. (2007). Spatial normalization of lesioned brains: Performance evaluation and impact on fMRI analyses. *NeuroImage*, *37*(3), 866–875.

Delis, D. C., Robertson, L. C., & Balliet, R. (1983). The breakdown and rehabilitation of visuospatial dysfunction in brain-injured patients. *International Rehabilitation Medicine*, *5*(3), 132–138.

Doricchi, F., & Galati, G. (2000). Implicit semantic evaluation of object symmetry and contralesional visual denial in a case of left unilateral neglect with damage of the dorsal paraventricular white matter. *Cortex*, *36*(3), 337–350.

Doricchi, F., Thiebaut de Schotten, M., Tomaiuolo, F., & Bartolomeo, P. (2008). White matter (dis)connections and gray matter (dys)functions in visual neglect: Gaining insights into the brain networks of spatial awareness. *Cortex*, *44*(8), 983–995.

Doricchi, F., & Tomaiuolo, F. (2003). The anatomy of neglect without hemianopia: A key role for parietal-frontal disconnection? *Neuroreport*, *14*(17), 2239–2243.

Duvernoy, H. M., Cabanis, E. A., & Vannson, J. L. (1991). *The human brain: Surface, three-dimensional sectional anatomy and MRI*. Wien, Austria: Springer-Verlag.

Friston, K. J., Ashburner, J., Frith, C. D., Poline, J. B., Heather, J. D., & Frackowiak, R. S. J. (1995). Spatial registration and normalization of images. *Human Brain Mapping*, *3*(3), 165–189.

Friston, K. J., Ashburner, J., Kiebel, S. J., Nichols, T. E., & Penny, W. (2007). *Statistical parametric mapping: The analysis of functional brain images* (1st ed.). Amsterdam, The Netherlands: Elsevier/Academic Press.

Gottesman, R. F., Kleinman, J. T., Davis, C., Heidler-Gary, J., Newhart, M., Kannan, V., et al. (2008). Unilateral neglect is more severe and common in older patients with right hemispheric stroke. *Neurology*, *71*(18), 1439–1444.

Halligan, P. W., & Marshall, J. C. (1994). Toward a principled explanation of unilateral neglect [Review]. *Cognitive Neuropsychology*, *11*(2), 167–206.

He, B. J., Snyder, A. Z., Vincent, J. L., Epstein, A., Shulman, G. L., & Corbetta, M. (2007). Breakdown of functional connectivity in frontoparietal networks underlies behavioral deficits in spatial neglect. *Neuron*, *53*(6), 905–918.

Heilman, K. M., & Valenstein, E. (1979). Mechanisms underlying hemispatial neglect. *Annals of Neurology*, *5*(2), 166–170.

Heinke, D., & Humphreys, G. W. (2003). Attention, spatial representation, and visual neglect: Simulating emergent attention and spatial memory in the selective attention for identification model (SAIM). *Psychological Review*, *110*(1), 29–87.

Hillis, A. E., Newhart, M., Heidler, J., Barker, P. B., Herskovits, E. H., & Degaonkar, M. (2005). Anatomy of spatial attention: Insights from perfusion imaging and hemispatial neglect in acute stroke. *Journal of Neuroscience*, *25*(12), 3161–3167.

Humphreys, G. W. (1998). Neural representation of objects in space: A dual coding account. *Philosophical Transactions of the Royal Society of London. Series B, Biological Sciences*, *353*(1373), 1341–1351.

Humphreys, G. W., & Riddoch, M. J. (1994). Attention to within-object and between-object spatial representations—multiple sites for visual selection. *Cognitive Neuropsychology*, *11*(2), 207–241.

Humphreys, G. W., & Riddoch, M. J. (1995). Separate coding of space within and between perceptual objects—evidence from unilateral visual neglect. *Cognitive Neuropsychology*, *12*(3), 283–311.

Karnath, H. O. (2001). New insights into the functions of the superior temporal cortex. *Nature Reviews Neuroscience*, *2*(8), 568–576.

Karnath, H. O., Ferber, S., & Himmelbach, M. (2001). Spatial awareness is a function of the temporal not the posterior parietal lobe. *Nature*, *411*(6840), 950–953.

Karnath, H. O., Fruhmann Berger, M., Kuker, W., & Rorden, C. (2004a). The anatomy of spatial neglect based on voxelwise statistical analysis: A study of 140 patients. *Cerebral Cortex*, *14*(10), 1164–1172.

Karnath, H. O., Fruhmann Berger, M., Zopf, R., & Kuker, W. (2004b). Using SPM normalization for lesion analysis in spatial neglect. *Brain*, *127*(4), E10; author reply, E11.

Karnath, H. O., Himmelbach, M., & Rorden, C. (2002). The subcortical anatomy of human spatial

neglect: Putamen, caudate nucleus and pulvinar. *Brain*, *125*(2), 350–360.

Karnath, H. O., Rorden, C., & Ticini, L. F. (2009). Damage to white matter fiber tracts in acute spatial neglect. *Cerebral Cortex*, *19*(10), 2331–2337.

Karnath, H. O., Zopf, R., Johannsen, L., Fruhmann Berger, M., Nagele, T., & Klose, U. (2005). Normalized perfusion MRI to identify common areas of dysfunction: Patients with basal ganglia neglect. *Brain*, *128*(10), 2462–2469.

Kleinman, J. T., Newhart, M., Davis, C., Heidler-Gary, J., Gottesman, R. F., & Hillis, A. E. (2007). Right hemispatial neglect: Frequency and characterization following acute left hemisphere stroke. *Brain and Cognition*, *64*(1), 50–59.

Leibovitch, F. S., Black, S. E., Caldwell, C. B., Ebert, P. L., Ehrlich, L. E., & Szalai, J. P. (1998). Brain–behavior correlations in hemispatial neglect using CT and SPECT: The Sunnybrook Stroke Study. *Neurology*, *50*(4), 901–908.

Maldjian, J. A., Laurienti, P. J., Kraft, R. A., & Burdette, J. H. (2003). An automated method for neuroanatomic and cytoarchitectonic atlas-based interrogation of fMRI data sets. *NeuroImage*, *19*(3), 1233–1239.

Mannan, S. K., Mort, D. J., Hodgson, T. L., Driver, J., Kennard, C., & Husain, M. (2005). Revisiting previously searched locations in visual neglect: Role of right parietal and frontal lesions in misjudging old locations as new. *Journal of Cognitive Neuroscience*, *17*(2), 340–354.

Marsh, E. B., & Hillis, A. E. (2008). Dissociation between egocentric and allocentric visuospatial and tactile neglect in acute stroke. *Cortex*, *44*(9), 1215–1220.

Mavritsaki, E., Allen, H. A., & Humphreys, G. W. (2010). Decomposing the neural mechanisms of visual search through model-based analysis of fMRI: Top-down excitation, active ignoring and the use of saliency by the right TPJ. *NeuroImage*, *52*(3), 934–946.

Mavritsaki, E., Heinke, D., Deco, G., & Humphreys, G. W. (2009). Simulating posterior parietal damage in a biologically plausible framework: Neuropsychological tests of the search over time and space model. *Cognitive Neuropsychology*, *26*(4), 343–390.

Medina, J., Kannan, V., Pawlak, M. A., Kleinman, J. T., Newhart, M., Davis, C., et al. (2009). Neural substrates of visuospatial processing in distinct reference frames: Evidence from unilateral spatial neglect. *Journal of Cognitive Neuroscience*, *21*(11), 2073–2084.

Mori, S. (2005). *MRI atlas of human white matter*. Amsterdam, The Netherlands: Elsevier.

Mort, D. J., Malhotra, P., Mannan, S. K., Pambakian, A., Kennard, C., & Husain, M. (2004). Reply to: Using SPM normalization for lesion analysis in spatial neglect [Letter]. *Brain*, *127,* E11.

Mort, D. J., Malhotra, P., Mannan, S. K., Rorden, C., Pambakian, A., Kennard, C., et al. (2003). The anatomy of visual neglect. *Brain*, *126*(9), 1986–1997.

Nichols, T., Brett, M., Andersson, J., Wager, T., & Poline, J. B. (2005). Valid conjunction inference with the minimum statistic. *NeuroImage*, *25*(3), 653–660.

Olson, C. R. (2003). Brain representation of object-centered space in monkeys and humans. *Annual Review of Neuroscience*, *26,* 331–354.

Ota, H., Fujii, T., Suzuki, K., Fukatsu, R., & Yamadori, A. (2001). Dissociation of body-centered and stimulus-centered representations in unilateral neglect. *Neurology*, *57*(11), 2064–2069.

Pajevic, S., & Pierpaoli, C. (1999). Color schemes to represent the orientation of anisotropic tissues from diffusion tensor data: Application to white matter fiber tract mapping in the human brain. *Magnetic Resonance in Medicine*, *42*(3), 526–540.

Riddoch, M. J., & Humphreys, G. W. (1983). The effect of cueing on unilateral neglect. *Neuropsychologia*, *21*(6), 589–599.

Riddoch, M. J., Humphreys, G. W., Luckhurst, L., Burroughs, E., & Bateman, A. (1995). Paradoxical neglect—spatial representations, hemisphere-specific activation, and spatial cueing. *Cognitive Neuropsychology*, *12*(6), 569–604.

Rorden, C., Fruhmann Berger, M., & Karnath, H. O. (2006). Disturbed line bisection is associated with posterior brain lesions. *Brain Research*, *1080*(1), 17–25.

Rorden, C., Karnath, H. O., & Bonilha, L. (2007). Improving lesion-symptom mapping. *Journal of Cognitive Neuroscience*, *19*(7), 1081–1088.

Salmond, C. H., Ashburner, J., Vargha-Khadem, F., Connelly, A., Gadian, D. G., & Friston, K. J. (2002). Distributional assumptions in voxel-based morphometry. *NeuroImage*, *17*(2), 1027–1030.

Salmond, C. H., Menon, D. K., Chatfield, D. A., Williams, G. B., Pena, A., Sahakian, B. J., et al. (2006). Diffusion tensor imaging in chronic head injury survivors: Correlations with learning and memory indices. *NeuroImage*, *29*(1), 117–124.

Smith, S. M., Jenkinson, M., Woolrich, M. W., Beckmann, C. F., Behrens, T. E., Johansen-Berg,

H., et al. (2004). Advances in functional and structural MR image analysis and implementation as FSL. *NeuroImage*, *23*(Suppl. 1), S208–S219.

Stamatakis, E. A., & Tyler, L. K. (2005). Identifying lesions on structural brain images—validation of the method and application to neuropsychological patients. *Brain and Language*, *94*(2), 167–177.

Thiebaut de Schotten, M., Kinkingnehun, S., Delmaire, C., Lehericy, S., Duffau, H., Thivard, L., et al. (2008). Visualization of disconnection syndromes in humans. *Cortex*, *44*(8), 1097–1103.

Thiebaut de Schotten, M., Urbanski, M., Duffau, H., Volle, E., Levy, R., Dubois, B., et al. (2005). Direct evidence for a parietal-frontal pathway subserving spatial awareness in humans. *Science*, *309*(5744), 2226–2228.

Thomas, C., Avidan, G., Humphreys, K., Jung, K. J., Gao, F., & Behrmann, M. (2009). Reduced structural connectivity in ventral visual cortex in congenital prosopagnosia. *Nature Neuroscience*, *12*(1), 29–31.

Urbanski, M., Thiebaut de Schotten, M., Rodrigo, S., Catani, M., Oppenheim, C., Touze, E., et al. (2008). Brain networks of spatial awareness: Evidence from diffusion tensor imaging tractography. *Journal of Neurology, Neurosurgery, and Psychiatry*, *79*(5), 598–601.

Vallar, G. (2001). Extrapersonal visual unilateral spatial neglect and its neuroanatomy. *NeuroImage*, *14*(1, Pt. 2), S52–S58.

Vallar, G., Bottini, G., & Paulesu, E. (2003). Neglect syndromes: The role of the parietal cortex. *Advances in Neurology*, *93,* 293–319.

Verdon, V., Schwartz, S., Lovblad, K. O., Hauert, C. A., & Vuilleumier, P. (2010). Neuroanatomy of hemispatial neglect and its functional components: A study using voxel-based lesion-symptom mapping. *Brain*, *133*(Pt. 3), 880–894.

Walker, R., Findlay, J. M., Young, A. W., & Lincoln, N. B. (1996). Saccadic eye movements in object-based neglect. *Cognitive Neuropsychology*, *13,* 569–615.

Walker, R., & Young, A. W. (1996). Object-based neglect: An investigation of the contributions of eye movements and perceptual completion. *Cortex*, *32*(2), 279–295.

Woolsey, T. A., Hanaway, J., & Gado, M. H. (2008). *The brain atlas: A visual guide to the human central nervous system* (3rd ed.). Hoboken, NJ: Wiley.

Worsley, K. J. (2003). Developments in random field theory. In R. S. J. Frackowiak, K. J. Friston, C. Frith, R. Dolan, C. J. Price, S. Zeki, J. Ashburner, & W. D. Penny (Eds), *Human brain function* (2nd ed., pp. 881–886). San Diego, CA: Academic Press.

APPENDIX A

Patient details: Clinical and demographic data

ID	*Sex/Age/ Handedness*	*Aetiology*	*Time post lesion (years)*	*Lesion side*	*VFD*	*Apple Cancellation score(/50)*[c]	*Asymmetry score: Full apples*[c]	*Asymmetry score: Incomplete apples*[c]	*Apple test/ retest*	*Nonword reading*
P1	M/55/R	S	4	B	—	46	2	0	0 (0)	0 (0)
P2	M/60/R	S	12	R	—	47	0	0	0 (0)	0 (0)
P3	F/81/R	S	10	R	—	50	0	0	0 (0)	0 (0)
P4	M/63/R	S	5	B	—	**22**	**22**	**2**	1 (1)	1 (1)
P5	F/65/R	CBD	4	B	—	**10**	**10**	**3**	1 (1)	1 (1)
P6	M/71/R	S	14	L	—	50	0	0	0 (0)	0 (0)
P7[a]	M/38/R	CM	12	R	—	49	0	0	0 (0)	0 (0)
P8[a]	M/70/R	CM	12	B	—	50	0	0	0 (0)	0 (0)
P9	M/52/R	HSE[b]	15	R	—	50	0	0	0 (0)	0 (0)
P10	M/66/R	S	18	B	+ (L)	**14**	**14**	**4**	1 (1)	1 (1)
P11	M/85/R	S	26	B	—	50	0	0	0 (0)	0 (0)
P12	F/63/L	S	3	R	+ (R)	45	3	0	0 (1)	0 (1)
P13	F/72/R	S	4	B	—	50	0	**4**	0 (1)	0 (1)
P14	F/57/R	S	2	L	—	**35**	0	0	1 (0)	1 (0)
P15	M/62/R	CBD	3	R	—	50	0	0	0 (0)	0 (0)
P16	M/61/R	S	5	R	—	50	0	0	0 (0)	0 (0)
P17	M/76/R	S	3	R	—	50	0	1	0 (0)	0 (0)
P18	M/69/R	S	4	R	—	**32**	**18**	**3**	1 (1)	1 (1)
P19	F/60/R	S	1	R	—	44	3	0	0 (0)	0 (0)
P20	M/65/R	S	2	R	—	**32**	**9**	1	NT	NT
P21	M/64/R	S	1	R	—	**40**	**10**	**4**	1 (1)	1 (1)
P22[a]	M/54/L	CM	10	L	—	50	0	**−4**	0 (1)	0 (0)
P23	F/81/R	S	1	L	—	**32**	**-18**	−1	NT	NT
P24	M/61/L	S	12	R	+ (L)	**40**	**9**	1	1 (1)	1 (1)
P25	M/48/R	S	5	R	—	50	0	0	NT	0 (0)
P26	M/75/R	S	3	L	+ (R)	**36**	0	0	1 (0)	1 (0)
P27	M/32/R	S	1	L	—	49	1	0	NT	NT
P28	M/32/R	S	2	R	—	49	1	0	NT	NT
P29	F/60/R	S	13	B	—	47	1	**7**	0 (1)	0 (1)
P30	M/34/R	S	9	L	—	50	0	0	0 (0)	NT
P31	M/72/R	S	4	L	—	50	0	0	0 (0)	NT
P32	M/72/R	S	7	R	—	50	0	0	0 (0)	0 (0)
P33	M/63/R	CBD[b]	3	B	—	**18**	**-18**	**5**	1 (1)	1 (1)
P34	M/53/R	S	3	R	—	47	3	**9**	1 (1)	1 (1)
P35	M/73/R	S	8	R	—	50	0	**−8**	0 (1)	0 (1)
P36	M/64/L	S	1	R	—	47	3	**2**	0 (0)	0 (0)

(*Continued overleaf*)

Appendix. (Continued)

ID	*Sex/Age/ Handedness*	*Aetiology*	*Time post lesion (years)*	*Lesion side*	*VFD*	*Apple Cancellation score(/50)*[c]	*Asymmetry score: Full apples*[c]	*Asymmetry score: Incomplete apples*[c]	*Apple test/ retest*	*Nonword reading*
P37	M/73/L	S	8	L	—	44	**4**	1	0 (0)	0 (0)
P38	F/58/R	S	4	B	—	50	0	0	0 (0)	0 (0)
P39	M/55/R	HSE[b]	10	B	—	50	0	0	0 (0)	0 (0)
P40	M/70/R	S	7	R	—	**38**	**12**	**4**	1 (1)	1 (1)
P41	F/78/R	S	1	R	—	**36**	0	0	0 (0)	0 (0)

Note: M = male; F = female; L = left; R = right; B = bilateral; S = stroke; CBD = cortico-basal degeneration; CM = carbon monoxide poisoning; HSE = herpes simplex encephalitis; VFD = visual field deficits; NT = not tested. Egocentric neglect is determined by whether patients miss targets (complete apples) on the left or right side of the page. Allocentric neglect is determined by whether patients make false-positive responses by cancelling incomplete apples (distractors) where the gap is on either the right or the left side of each apple, irrespective of the position of the (incomplete) apple on the page. Cut-offs to classify patients as having egocentric or allocentric neglect were calculated on the basis of asymmetry scores (left- vs. right-side egocentric or allocentric errors), using scores from 86 elderly control participants, and were as follows: Egocentric asymmetry for full apples (based on <2.5th percentile) 3 left-side errors; allocentric asymmetry for incomplete apples (based on <2.5th percentile) 1 left-side errors. The cut-off for total numbers of target omissions (i.e., accuracy score) was 40/50 (based on <2.5th percentile). Scores where there is a clinical deficit are highlighted in bold. On the Apple test/retest score we note whether a patient had a clinical deficit when retested for egocentric (allocentric, in parentheses) neglect. 1 = a clinical deficit, 0 = within-test norms. The nonword reading test required patients to read aloud 40 randomly positioned pronounceable nonwords on an A4 sheet. A clinical deficit of egocentric neglect was based on 2.5th percentile cut-off on data from 20 elderly control participants (ages 60–75 years). Egocentric neglect was classified as omitting 2 more nonwords on one side of the page than on the other. Allocentric neglect was classified as making, across the nonwords attempted, 2 more errors at one end of the strings than at the other. 1 = a clinical deficit, 0 = no deficit for egocentric (and allocentric, in parentheses) neglect. For the measure of egocentric neglect from the Apples test there was 89% concordance between the classification derived from the test/retest scores, and an 89% concordance also for the egocentric neglect measures from the Apples test and the nonword reading test. For the measure of allocentric neglect from the Apples test there was 94% concordance between the classification achieved from test/retest scores and also 94% concordance between the Apples test score and the measure of allocentric neglect in the nonword reading task.

[a]Three patients with carbon monoxide poisoning who were excluded from the final analysis (see Method section and Footnote 2 for further details). [b]Patients with chronic degenerative changes who were presented with additional acquired brain lesions resulting from unspecified vascular disease. [c]The maximum achievable score in the Apple Cancellation Task is 50.

APPENDIX B

Examples of segmentation and lesion reconstruction

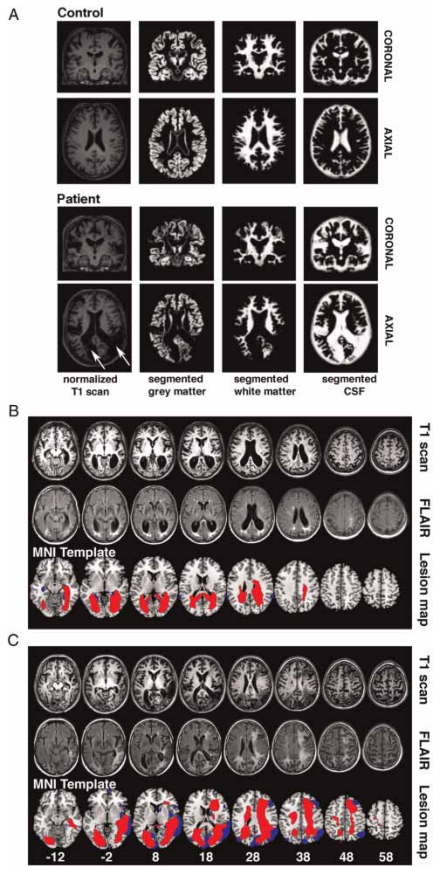

Figure B1. *(A) Illustration of the output of the advanced segment–normalize procedure applied to high-resolution T1-weighted MRI scans from one of the healthy control participants (67-year-old male) and one of the neglect patients (63-year-old male with left egocentric neglect and left allocentric neglect). This procedure (see Method for full details) involves tissue classification based on the signal intensity in each voxel and on a priori knowledge of the expected localization of grey matter, white matter, and cerebrospinal fluid (CSF). The outputs of this procedure are three classified tissue maps representing the probability that a given voxel "belongs" to a specific tissue class. The brain tissue affected by stroke (white arrows) is typically mapped with reduced likelihood of representing either grey or white matter due to the change in signal intensities caused by stroke. In the current study we tested only chronic patients, and thus in majority of cases the region of the damaged tissue was "replaced"/"filled" by CSF as shown here. (B, C) Illustration of the reconstructed lesion maps and corresponding T1 and FLAIR (fluid-attenuated inversion recovery) scans from two of the neglect patients with degenerative changes (B: 65-year-old female with left egocentric neglect and left allocentric neglect; C: 63-year-old male with right egocentric neglect and left allocentric neglect). The bottom row shows binary map of grey matter (dark grey; displayed in blue in the online figure) and white matter (light grey; displayed in red in the online figure) lesions. The binary lesion map is presented as an overlay on a standard T1 multislice template in MRIcron (Rorden, 2007, University of South Carolina, Columbia, SC, USA, Retrieved August 1, 2010, from http://www.cabiatl.com/mricro/mricron/index.html). MNI z-coordinates of the axial sections are given. For all patients reconstructed lesion maps were verified against the high-resolution T1 scans (where available, we also used T2 or FLAIR contrasts, in particular in the case of patients with degenerative changes as shown here), and these lesion maps were further used in VLSM (voxel-based lesion symptom mapping) analysis (see Method for full details). All images in (A), (B), and (C) are displayed in neurological convention—that is, left of the slice represents the left hemisphere. To view a colour version of this figure, please see the online issue of the Journal.*

APPENDIX C

Normalized behavioural scores used as covariates in all voxel-wise analyses of neuroimaging data

	Neglect score			
	Allocentric		*Egocentric*	
ID	*Left*	*Right*	*Left*	*Right*
P1	0	0	0	0
P2	0	0	0	0
P3	0	0	0	0
P4	2	0	0.8	0
P5	3	0	0.25	0
P6	0	0	0	0
P7	0	0	0	0
P8	0	0	0	0
P9	0	0	0	0
P10	4	0	0.4	0
P11	0	0	0	0
P12	0	0	0	0
P13	4	0	0	0
P14	0	0	0	0
P15	0	0	0	0
P16	0	0	0	0
P17	0	0	0	0
P18	3	0	1	0
P19	0	0	0	0
P20	0	0	0.5	0
P21	4	0	1	0
P22	0	4	0	0
P23	0	0	0	1
P24	0	0	0.9	0
P25	0	0	0	0
P26	0	0	0	0
P27	0	0	0	0
P28	0	0	0	0
P29	7	0	0	0
P30	0	0	0	0
P31	0	0	0	0
P32	0	0	0	0
P33	5	0	0	0.6
P34	9	0	0	0
P35	0	8	0	0
P36	2	0	0	0
P37	0	0	0	0
P38	0	0	0	0
P39	0	0	0	0
P40	4	0	1	0
P41	0	0	0	0

Note: The behavioural scores used in the neuroimaging analyses were classified based on cut-offs drawn from the Birmingham University Cognitive Screen (BUCS; see Method section for full information). In addition, to account for variation in overall performance affected by general motor and attentional deficits, we divided the asymmetry score for full apples by the total number of full apples missed, and these scores were used respectively as left and right egocentric neglect covariates.